# Secular variability in zircon phosphorus concentrations prevents simple petrogenetic classification
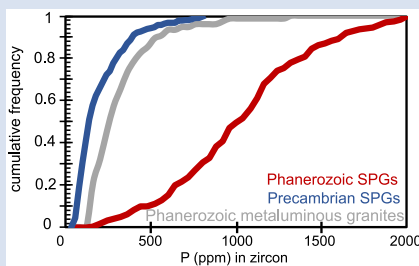
## C.E. Bucholz[1*], J. Liebmann[2], C.J. Spencer[3]

OPEN ACCESS

## Abstract



Phosphorus (P) concentrations in zircon have been used to discriminate their derivation from metaluminous *versus* strongly peraluminous granites (SPGs) based on the empirical observation of lower P concentrations in zircon from Phanerozoic metaluminous *versus* peraluminous granites. Higher P concentrations in zircon from Phanerozoic SPGs reflect enhanced apatite solubility in peraluminous melts and overall higher P concentrations in peraluminous granites. However, SPGs derived from partial melting of Precambrian sedimentary rocks have lower P concentrations compared to Phanerozoic metaluminous granites, reflecting lower P concentrations in Precambrian *versus* Phanerozoic sedimentary sources. We demonstrate that zircons from Precambrian SPGs also have lower P concentrations compared to Phanerozoic counterparts, likely reflecting lower P concentrations in their parental melts. Applying the P-in-zircon proxy to the detrital zircon record does not effectively discriminate between metaluminous and peraluminous sources and underestimates contributions from peraluminous granites. Although detrital zircons are an important early Earth archive, a uniformitarian perspective cannot always be applied when using trace element proxies developed on Phanerozoic samples.

## Introduction

Trace element concentrations in zircon are used to "fingerprint" the magma from which they crystallised (*e.g.*, Grimes *et al.*, 2015). Of particular interest is identification of zircon from "I-type" or metaluminous granites *versus* those from "S-type" or strongly peraluminous granites (SPGs[1]; Burnham and Berry, 2017; Trail *et al.*, 2017). Understanding the relative contribution of zircon from metaluminous *versus* peraluminous granites throughout Earth's history yields information on lithologic diversity and tectonic environments through time. SPGs dominantly form in collisional orogenic environments through the partial melting of sedimentary rocks (Nabelek, 2020). Thus, their inferred presence (or absence) through time yields information on both tectonic regimes and the availability of sedimentary rocks to be recycled into magmas during orogenic cycles.

One proposed proxy to discriminate zircon from metaluminous and peraluminous granites is phosphorus (P) concentrations in zircon (Burnham and Berry, 2017). As the solubility of apatite increases with melt aluminium saturation index (Pichavant *et al.*, 1992; Wolf and London, 1994), P concentrates in peraluminous melts during differentiation due to the lack of apatite precipitation (Bea *et al.*, 1994), a trend contrary to that observed in metaluminous melts (Lee and Bachmann, 2014).

Indeed, Phanerozoic SPGs have significantly higher $P_2O_5$ (on average ~0.25 wt. % and up to ~1.5 wt. % $P_2O_5$; Bea *et al.*, 1992; Bucholz, 2022; Fig. 1a,b) than metaluminous granites (which generally have <0.20 wt. % at bulk rock $SiO_2$ > 65 wt. %). Further, upon apatite saturation, P concentrations are buffered at higher levels in peraluminous than metaluminous melts.

Consequently, assuming equivalent zircon-melt P partition coefficients for metaluminous and peraluminous granitic systems, zircons from SPGs should have higher P contents than those from metaluminous granitic melts (Burnham and Berry, 2017). Indeed, P in zircons from Phanerozoic peraluminous *versus* metaluminous granites have higher P concentrations (means of $1017 \pm 53$ *versus* $312 \pm 48$ ppm (2 s.e.); Burnham and Berry, 2017; Zhu *et al.*, 2020; Fig. 1c,d). Further, P and REE + Y concentrations are strongly correlated in zircon from Palaeozoic SPGs, suggesting the incorporation of P, REE, and Y into the zircon lattice *via* the coupled xenotime-type mechanism $[(Y, REE)^{3+} + P^{5+} = Zr^{4+} + Si^{4+}]$. Based on these observations it has been proposed that P > 750 ppm and (REE + Y) < 1.15*P are robust criteria for identifying zircon from peraluminous granites (Burnham and Berry, 2017).

However, $P_2O_5$ concentrations in SPGs are not elevated above those of metaluminous granites throughout Earth history

1. Division of Geological and Planetary Sciences, California Institute of Technology, Pasadena, CA 91125
2. School of Earth and Planetary Sciences, Curtin University, 6845, Perth, Australia 6845
3. Department of Geological Sciences and Geological Engineering, Queen's University, Kingston, Canada K7L 3N6
* Corresponding author (email: cbucholz@caltech.edu)

1. We prefer the use of strongly peraluminous granite over "S-type" granites as the former is purely a geochemical definition that avoids confusion associated with the "alphabet" granite classification scheme (*c.f.*, Frost *et al.*, 2001). However, we emphasise that the SPGs discussed here have all been previously demonstrated to have formed *via* the partial melting of metasedimentary rocks.
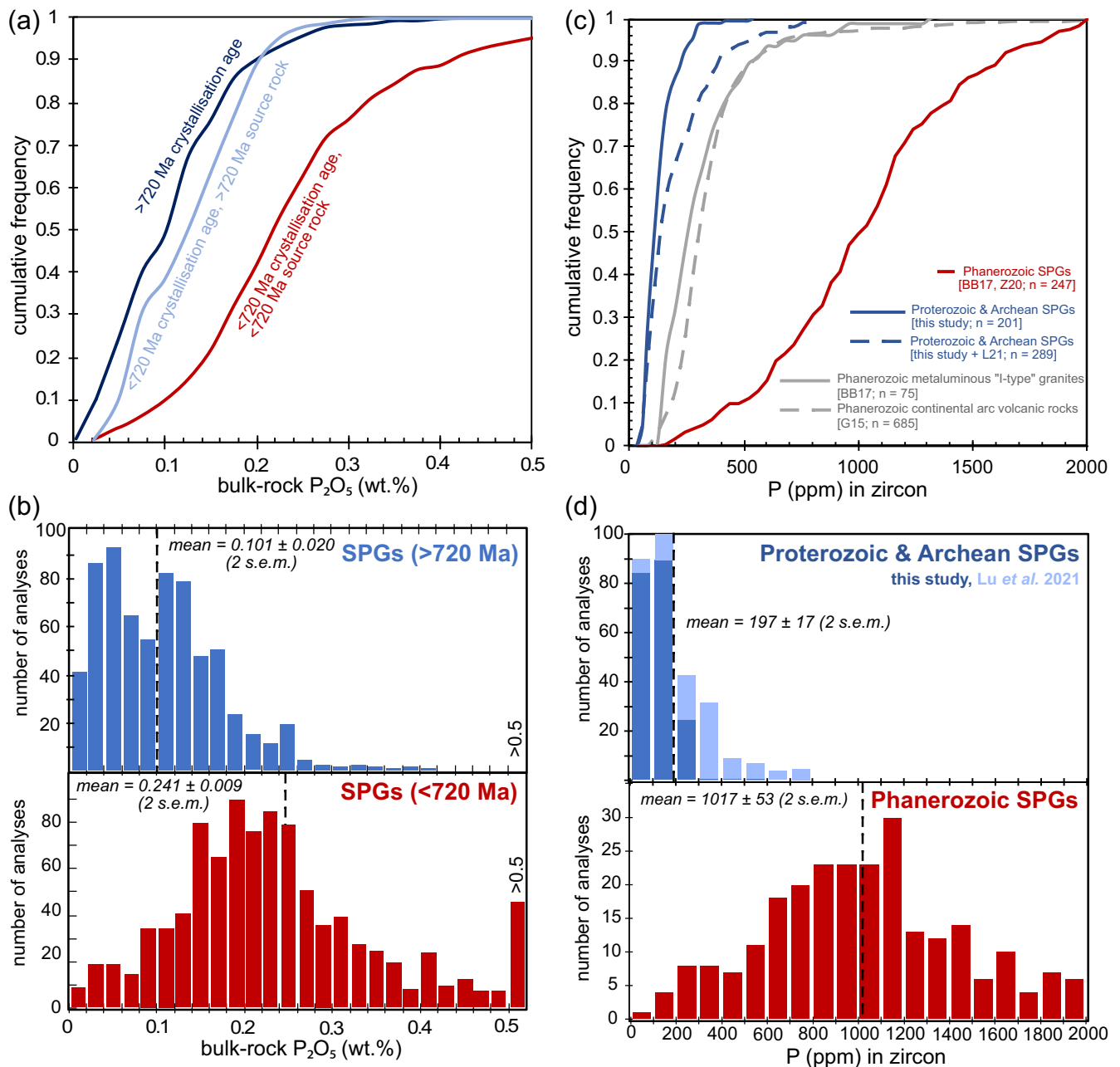
**Figure 1** **(a)** Cumulate frequency distributions of SPG bulk rock $P_2O_5$. **(b)** Histograms of SPG bulk rock $P_2O_5$ with source rock and crystallisation ages >720 Ma (top) and <720 Ma (bottom). Data in **(a)** and **(b)** from Bucholz (2022). **(c)** Cumulative frequency distributions of P in zircon for Proterozoic and Archean SPGs, as well as Phanerozoic SPGs, "I-type" granites, and continental arc volcanic rocks. **(d)** Histograms of zircon P concentrations for Proterozoic/Archean SPGs and Phanerozoic SPGs. Phanerozoic SPG and I-type granite data in **(c)** and **(d)** are from Burnham and Berry (2017) and Zhu et al. (2020) and continental arc volcanic zircon from Grimes et al. (2015).

(Bucholz, 2022). Maximum and average $P_2O_5$ concentrations in SPGs derived from sedimentary rocks deposited after 720 Ma are elevated above those derived from older source rocks (Fig. 1a,b). This temporal variation mirrors a similar increase in P concentrations in marine siliciclastic sediments deposited after 720 Ma, related to increased atmospheric and marine $O_2$ levels and enhanced authigenic P burial (Reinhard et al., 2017). After considering the factors affecting P concentrations in SPGs, Bucholz (2022) concluded that the temporal change in P concentrations is most likely explained as reflecting higher P concentrations in younger sedimentary source rocks. Elevated P concentrations in SPGs derived from sedimentary rocks deposited after 720 Ma could reflect both higher melt P concentrations

and/or inherited P-rich restitic minerals (e.g., apatite, monazite, or P-bearing silicates).

If P concentrations in Archean and most Proterozoic SPGs are relatively low and if this, to some degree, represents lower melt P concentrations, zircon crystallising from such melts may record these low P concentrations. To test this hypothesis, we analysed trace element concentrations (including P) in zircon from Meso- to Paleoproterozoic and Archean SPGs.

## Studied Samples and Methods

We analysed trace elements in zircon (n = 201 analyses) from 16 previously characterised SPGs (Liebmann et al., 2021a,b) from

the southwestern USA (*ca.* 1.4 Ga), the North China Craton (*ca.* 1.9 and 2.5 Ga), Finland (*ca.* 1.8–1.9 Ga), and Ghana (*ca.* 2.2 Ga) (see Tables S-1 and S-2 for locality, lithologic, and bulk rock major elements). The average bulk rock $P_2O_5$ contents of these SPGs are 0.088 ± 0.036 wt. % (2 s.e.). U-Pb isotopes and trace elements (Ca, P, Y, Hf, and REEs) were collected simultaneously using split stream laser ablation inductively coupled plasma mass spectrometry at UC Santa Barbara. Full analytical details are given in the Supplementary Information (SI) and sample and standard analyses are given in Tables S-4 and S-5, respectively. Cathodoluminescence imaging and U-Pb ages were used to ensure analysis of magmatic zircon (*i.e.* related to the crystallisation of the SPG) and not inherited cores/grains (Fig. S-1). Any analyses of inherited cores (with older U-Pb ages) or with >5 % discordance of U-Pb ages were excluded. No apatite inclusions were observed. We are aware of only one other locality of >720 Ma SPGs where trace elements in magmatic zircon were analysed (Lu *et al.*, 2021) and include these data in our discussion.

## Results

The P concentrations in Archean and Proterozoic SPGs are positively skewed (average = 132 ± 10 (2 s.e.) ppm; median = 110 ppm; and including Lu *et al.* (2021) data, average = 196 ± 17 ppm; median = 138 ppm). In comparison, P concentrations in zircon from Phanerozoic SPGs are normally distributed with an average of 1017 ± 53 (2 s.e.) (Fig. 1c,d). Cumulative frequency distributions of P concentrations highlight this difference (Fig. 1c) and the mean P concentration in zircon from Precambrian and Phanerozoic SPGs are statistically distinguishable (P < 0.00001, Wilcoxon rank sum test). Zircon REE + Y concentrations from Precambrian SPGs, although weakly correlated with P ($R^2$ = 0.63), are defined by a slope of >1.15, distinct from the Phanerozoic SPG trend (Fig. 2). Neither P nor total REE concentrations correlate with Ca concentrations, suggesting that P concentrations are not reflecting the incorporation of apatite inclusions in the ablation volume.
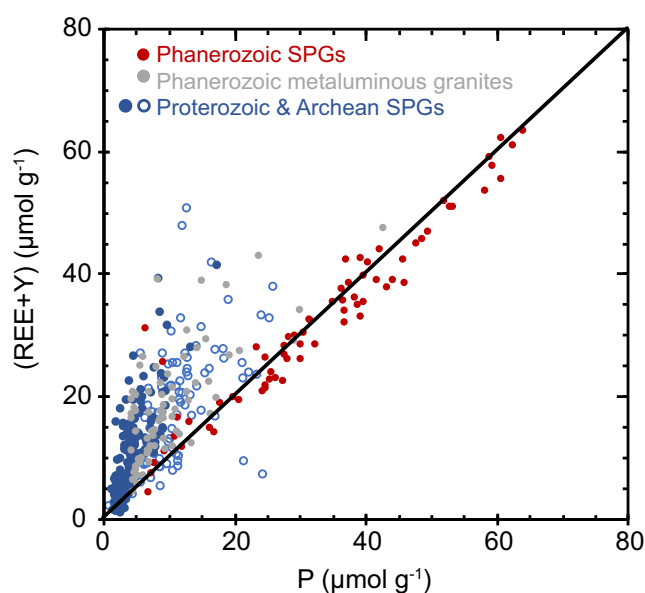


**Figure 2**   REE + Y *versus* P (in µmol/g) in zircon. Phanerozoic granite data are the same as in Figure 1. Proterozoic and Archean SPGs are from this study (filled symbols) and Lu *et al.* (2021) (open symbols).

## What Do Zircon P Concentrations Represent?

The P concentration of zircon reflects equilibrium and/or disequilibrium processes during crystallisation from melt, including (1) equilibrium partitioning dependent on temperature, pressure, and melt composition, (2) partitioning reflecting melt-crystal boundary layer concentrations controlled by diffusion of P in the melt, or (3) surface controlled non-equilibrium growth (*e.g.*, Watson and Liang, 1995; Hofmann *et al.*, 2009). In the first scenario, assuming that P partitioning is both Henrian and that equilibrium between zircon and melt occurred, then lower P concentrations in zircon from Archean/Proterozoic *versus* Phanerozoic SPGs could reflect either lower P concentrations in their parental melts or different conditions of crystallisation (*e.g.*, melt composition, pressure, and temperature) which resulted in variable zircon-melt P partition coefficients. Phosphorus partitioning between melt and zircon as a function of melt composition, temperature, and pressure is poorly understood with limited experimental studies available (Rubatto and Hermann, 2007; Taylor *et al.*, 2015). However, Archean/ Proterozoic SPGs are thought to have formed under similar conditions (*e.g.*, pressure, temperature) to those in the Phanerozoic (Bucholz and Spencer, 2019). Thus, in the first scenario of equilibrium partitioning, the simplest explanation is that lower P concentrations in zircon from Archean/Proterozoic SPGs, as compared to Phanerozoic ones, reflect lower melt P concentrations.

In the second scenario, the growth rate of zircon approaches (or exceeds) the diffusivity of P (and/or REE) in the adjacent melt. For hydrous rhyolites (~6 wt. % $H_2O$), experimentally calibrated P and Zr diffusivities (D) are similar with $\log(D_P)$ and $\log(D_{Zr})$ between −13.5 to −14.5 $m^2$/s at 750–850 °C (see review of Zhang and Gan, 2022). However, when zircon growth is sufficiently fast, P due to its general incompatibility is excluded from the zircon and builds up in a melt boundary layer. Thus, the growth of new zircon in equilibrium with this boundary layer acquires higher P concentrations elevated above that predicted by equilibrium partitioning with the bulk (*i.e.* far field) melt. However, all else being equal (*e.g.*, P diffusivity and partition coefficients), melts with higher bulk P concentrations would produce boundary layers with higher P concentrations which would be reflected in higher zircon P concentrations.

Finally, in the third scenario, unequivocal evidence for surface controlled, non-equilibrium growth manifests as sector zoning (Watson and Liang, 1995), however (sub-)µm scale oscillatory variations P concentrations have also been attributed to non-equilibrium growth (Hofmann *et al.*, 2009). We generally avoided analysing portions of zircon that exhibited sector zoning (Fig. S-1). However, when analysed, sector zoned zircon had similar P concentrations to other zircon from the sample (*c.f.*, 18IM15b; Fig. S-1). Further, the 25 µm laser spot used homogenised any visible oscillatory zoning (Fig. S-1), providing an integrated P concentration of the ablation volume. In zircon where multiple (2–3) spots were analysed, P concentrations agree within 25 ppm for 70 % and within 50 ppm for 80 % of zircon (Fig. S-3), suggesting that potential local variability induced by non-equilibrium growth was mostly homogenised.

No matter the P incorporation mechanism, our study demonstrates unequivocally that zircons from Archean and Proterozoic SPGs have lower P concentrations on average than their Phanerozoic SPGs (Figs. 1, 2). A parsimonious explanation for this observation is that lower P concentrations in zircons from Precambrian SPGs reflect lower P concentrations of their granitic parental melts. To explore this idea, we modelled melt $P_2O_5$ and
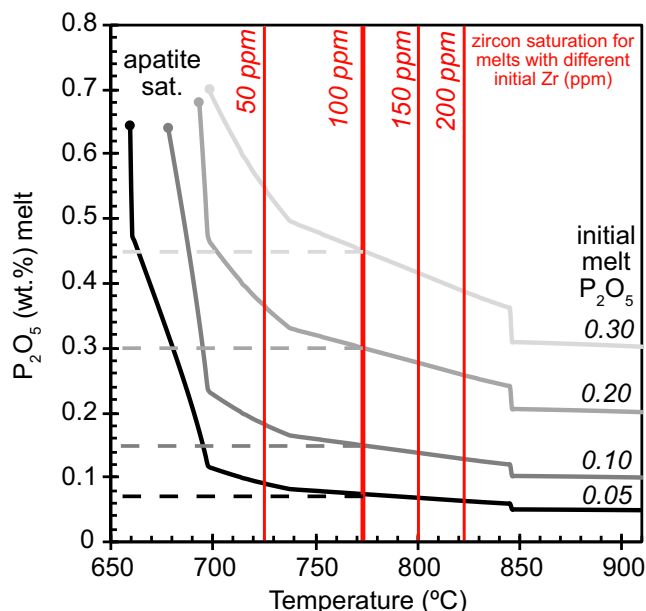
**Figure 3** Model results for melt $P_2O_5$ (wt. %) *versus* temperature during crystallisation of a SPG melt for different initial melt $P_2O_5$ (wt. %). Melt trajectories end once apatite saturation is reached. Zircon saturation temperatures are indicated with vertical red lines.

zircon and apatite saturation during crystallisation of a SPG melt using alphaMELTS (Pichavant *et al.*, 1992; Smith and Asimow, 2005; Boehnke *et al.*, 2013). Full modelling details are given in the SI. Calculations were performed for initial melt $P_2O_5$ contents typical of SPGs across Earth history (0.05, 0.10, 0.20, and 0.30 wt. %; Fig. 1a,b).

Due to compositional proximity to the granitic eutectic, zircon saturation temperatures were primarily controlled by increasing Zr concentrations in the melt with progressive differentiation. For initial Zr concentrations in the melt of 50, 100, 150, and 200 ppm, calculated zircon saturation temperatures are ~727, 772, 800, and 822 °C, respectively. [Average Zr concentrations of pre-720 Ma SPGs from Bucholz (2022) are $120 \pm 7$ ppm (2 s.e.).] The calculated saturation temperatures agree with calculated Ti-in-zircon temperatures which on average are $810 \pm 119$ °C and $741 \pm 105$ °C (2 s.d.) assuming a melt TiO$_2$ activity of 0.5 and 1, respectively (see SI for calculation details). For 100 ppm Zr in the initial melt, modelled melt $P_2O_5$ concentrations at zircon saturation are 0.08, 0.15, 0.30, and 0.45 wt. % for initial melt $P_2O_5$ contents of 0.05, 0.10, 0.20, and 0.30 wt. %, respectively (Fig. 3). Importantly, at zircon saturation, the melt $P_2O_5$ concentration has not significantly increased from its initial value as the melt fraction is still high (~75 %). For a melt with initially low $P_2O_5$ (0.05–0.10 wt. %) typical for Precambrian SPGs, melt $P_2O_5$ increases significantly only within 20–30 °C of the granitic eutectic when the melt fraction decreases dramatically. Calculated melts ultimately reach apatite saturation 70–110 °C below that of the zircon saturation for a melt with 100 ppm initial Zr (Fig. 3). Therefore, although melt $P_2O_5$ increases due to delayed apatite saturation in these peraluminous melts, it remains low at zircon saturation in SPG melts with initially low P contents.

## Implications and Conclusion

As SPGs predominantly form during collisional orogenesis, an accurate understanding of their temporal distribution provides information on the tectonic evolution and crustal recycling

through time (Bucholz and Spencer, 2019; Frost and Da Prat, 2021). Although detrital zircon can help characterise igneous rocks throughout Earth history, a uniformitarian approach cannot always be applied when using trace element proxies developed on Phanerozoic samples. Specifically, this study provides an example of how temporal variations in sedimentary rocks affect our interpretation of the igneous rock (and mineral) record. For example, the use of zircon P concentrations to identify metaluminous *versus* peraluminous source rocks has been applied to Archean and Hadean detrital zircon (Burnham and Berry, 2017; Zhu *et al.*, 2020). In particular, P and the correlation between P and REE + Y in Jack Hills zircon are more similar to Phanerozoic metaluminous granites and have been used to infer that the Jack Hills zircon crystallised from "TTG-like" magmas (Burnham and Berry, 2017). However, the nature of the source rocks for the Jack Hills zircon is debated with elevated $^{18}O/^{16}O$ ratios (Cavosie *et al.*, 2005; Trail *et al.*, 2007) and Al concentrations in Jack Hills zircon (Ackerson *et al.*, 2021), potentially indicating that some Jack Hills zircons are from granites with a sedimentary source. Our results demonstrate that low P contents and P/(Y + REE) values <1 in Precambrian zircons cannot rule out crystallisation from a peraluminous granitic melt. Therefore, low P contents in Jack Hills zircon is consistent with crystallisation from both metaluminous and peraluminous melts, supporting inferences that the Jack Hills zircon could be sourced from a variety of granitic magmas (Bell, 2017; Ackerson *et al.*, 2021).

Similarly, both cumulative distributions of P contents and P correlations with REE + Y in detrital zircons have been used to infer that SPG formation in the Archean was negligible and limited until the Neoproterozoic to Palaeozoic (Zhu *et al.*, 2020). However, we again urge caution about extrapolating these metrics to Precambrian zircon when sedimentary source regions of SPGs had low P concentrations. Further, Phanerozoic SPGs with sedimentary source rocks deposited before 720 Ma also have low P concentrations (Fig. 1a) and should also contain magmatic zircon with low P. However, P concentrations of detrital zircon may be useful in local studies of young terranes to identify contributions from Phanerozoic P-rich SPGs. Identification of detrital zircon from SPGs with Precambrian source rocks is perhaps best done through a combination of O isotopes with new developing zircon proxies such as Al concentrations (Ackerson *et al.*, 2021) or Si isotopes (Trail *et al.*, 2018).

## Additional Information

**Supplementary Information** accompanies this letter at https://www.geochemicalperspectivesletters.org/article2240.

## References

Ackerson, M.R., Trail, D., Buettner, J. (2021) Emergence of peraluminous crustal magmas and implications for the early Earth. *Geochemical Perspectives Letters* 17, 50–54. https://doi.org/10.7185/geochemlet.2114

Bea, F., Fershtater, G., Corretgé, L.G. (1992) The geochemistry of phosphorus in granite rocks and the effect of aluminium. *Lithos* 29, 43–56. https://doi.org/10.1016/0024-4937(92)90033-U

Bea, F., Pereira, M.D., Corretgé, L.G., Fershtater, G.B. (1994) Differentiation of strongly peraluminous, perphosphorus granites: The Pedrobernardo pluton, central Spain. *Geochimica et Cosmochimica Acta* 58, 2609–2627. https://doi.org/10.1016/0016-7037(94)90132-5

Bell, E. (2017) Ancient magma sources revealed. *Nature Geoscience* 10, 397–398. https://doi.org/10.1038/ngeo2955

Boehnke, P., Watson, E.B., Trail, D., Harrison, T.M., Schmitt, A.K. (2013) Zircon saturation re-revisited. *Chemical Geology* 351, 324–334. https://doi.org/10.1016/j.chemgeo.2013.05.028

Bucholz, C.E. (2022) Coevolution of sedimentary and strongly peraluminous granite phosphorus records. *Earth and Planetary Science Letters* 596, 117795. https://doi.org/10.1016/j.epsl.2022.117795

Bucholz, C.E., Spencer, C.J. (2019) Strongly Peraluminous Granites across the Archean–Proterozoic Transition. *Journal of Petrology* 60, 1299–1348. https://doi.org/10.1093/petrology/egz033

Burnham, A.D., Berry, A.J. (2017) Formation of Hadean granites by melting of igneous crust. *Nature Geoscience* 10, 457–461. https://doi.org/10.1038/ngeo2942

Cavosie, A.J., Valley, J.W., Wilde, S.A., E.I.M.F. (2005) Magmatic δ18O in 4400–3900 Ma detrital zircons: A record of the alteration and recycling of crust in the Early Archean. *Earth and Planetary Science Letters* 235, 663–681. https://doi.org/10.1016/j.epsl.2005.04.028

Frost, C.D., Da Prat, F.A. (2021) Petrogenetic and tectonic interpretation of strongly peraluminous granitic rocks and their significance in the Archean rock record. *American Mineralogist* 106, 1195–1208. https://doi.org/10.2138/am-2022-8001

Grimes, C.B., Wooden, J.L., Cheadle, M.J., John, B.E. (2015) "Fingerprinting" tectono-magmatic provenance using trace elements in igneous zircon. *Contributions to Mineralogy and Petrology* 170, 46. https://doi.org/10.1007/s00410-015-1199-3

Hofmann, A.E., Valley, J.W., Watson, E.B., Cavosie, A.J., Eiler, J.M. (2009) Submicron scale distributions of trace elements in zircon. *Contributions to Mineralogy and Petrology* 158, 317–335. https://doi.org/10.1007/s00410-009-0385-6

Lee, C.-T.A., Bachmann, O. (2014) How important is the role of crystal fractionation in making intermediate magmas? Insights from Zr and P systematics. *Earth and Planetary Science Letters* 393, 266–274. https://doi.org/10.1016/j.epsl.2014.02.044

Liebmann, J., Spencer, C.J., Kirkland, C.L., Bucholz, C., He, X., Santosh, M., Xia, X.P., Martin, L., Evans, N.J. (2021a) Emergence of continents above sea-level influences sediment melt composition. *Terra Nova* 33, 465–474. https://doi.org/10.1111/ter.12531

Liebmann, J., Spencer, C.J., Kirkland, C.L., Bucholz, C.E., Xia, X.-P., Martin, L., Kitchen, N., Shumlyanskyy, L. (2021b) Coupling sulfur and oxygen isotope ratios in sediment melts across the Archean-Proterozoic transition. *Geochimica et Cosmochimica Acta* 307, 242–257. https://doi.org/10.1016/j.gca.2021.05.045

Lu, G.-M., Spencer, C.J., Tian, Y., Wang, W. (2021) Significant Increase of Continental Freeboard During the Early Paleoproterozoic: Insights From Metasediment-Derived Granites. *Geophysical Research Letters* 48, e2021GL096049. https://doi.org/10.1029/2021GL096049

Nabelek, P.I. (2020) Petrogenesis of leucogranites in collisional orogens. *Geological Society, London, Special Publications* 491, 179–207. https://doi.org/10.1144/SP491-2018-181

Pichavant, M., Montel, J.-M., Richard, L.R. (1992) Apatite solubility in peraluminous liquids: Experimental data and an extension of the Harrison-Watson model. *Geochimica et Cosmochimica Acta* 56, 3855–3861. https://doi.org/10.1016/0016-7037(92)90178-L

Reinhard, C.T., Planavsky, N.J., Gill, B.C., Ozaki, K., Robbins, L.J., Lyons, T.W., Fischer, W.W., Wang, C., Cole, D.B. and Konhauser, K.O. (2017) Evolution of the global phosphorus cycle. *Nature* 541, 386–389. https://doi.org/10.1038/nature20772

Rubatto, D., Hermann, J. (2007) Experimental zircon/melt and zircon/garnet trace element partitioning and implications for the geochronology of crustal rocks. *Chemical Geology* 241, 38–61. https://doi.org/10.1016/j.chemgeo.2007.01.027

Smith, P.M., Asimow, P.D. (2005) Adiabat_1ph: A new public front-end to the MELTS, pMELTS, and pHMELTS models: ADIABAT_1PH FRONT-END. *Geochemistry, Geophysics, Geosystems* 6. https://doi.org/10.1029/2004GC000816

Taylor, R.J.M., Harley, S.L., Hinton, R.W., Elphick, S., Clark, C., Kelly, N.M. (2015) Experimental determination of REE partition coefficients between zircon, garnet and melt: a key to understanding high-*T* crustal processes. *Journal of Metamorphic Geology* 33, 231–248. https://doi.org/10.1111/jmg.12118

Trail, D., Mojzsis, S.J., Harrison, T.M., Schmitt, A.K., Watson, E.B., Young, E.D. (2007) Constraints on Hadean zircon protoliths from oxygen isotopes, Ti-thermometry, and rare earth elements. *Geochemistry, Geophysics, Geosystems* 8, Q06014. https://doi.org/10.1029/2006GC001449

Trail, D., Tailby, N., Wang, Y., Mark Harrison, T., Boehnke, P. (2017) Aluminum in zircon as evidence for peraluminous and metaluminous melts from the Hadean to present. *Geochemistry, Geophysics, Geosystems* 18, 1580–1593. https://doi.org/10.1002/2016GC006794

Trail, D., Boehnke, P., Savage, P.S., Liu, M.-C., Miller, M.L., Bindeman, I. (2018) Origin and significance of Si and O isotope heterogeneities in Phanerozoic, Archean, and Hadean zircon. *Proceedings of the National Academy of Sciences* 115, 10287–10292. https://doi.org/10.1073/pnas.1808335115

Watson, E.B., Liang, Y. (1995) A simple model for sector zoning in slowly grown crystals; implications for growth rate and lattice diffusion, with emphasis on accessory minerals in crustal rocks. *American Mineralogist* 80, 1179–1187. https://doi.org/10.2138/am-1995-11-1209

Wolf, M.B., London, D. (1994) Apatite dissolution into peraluminous haplogranitic melts: An experimental study of solubilities and mechanisms. *Geochimica et Cosmochimica Acta* 58, 4127–4145. https://doi.org/10.1016/0016-7037(94)90269-0

Zhang, Y., Gan, T. (2022) Diffusion in Melts and Magmas. *Reviews in Mineralogy and Geochemistry* 87, 283–337. https://doi.org/10.2138/rmg.2022.87.07

Zhu, Z., Campbell, I.H., Allen, C.M., Burnham, A.D. (2020) S-type granites: Their origin and distribution through time as determined from detrital zircons. *Earth and Planetary Science Letters* 536, 116140. https://doi.org/10.1016/j.epsl.2020.116140